Applied Thermal Engineering 31 (2011) 2819–2828

Contents lists available at ScienceDirect

Applied Thermal Engineering

journal homepage: www.elsevier.com/locate/apthermeng

A numerical study on thermo-hydraulic characteristics of turbulent flow in a circular tube fitted with conical strip inserts

Aiwu Fan, Junjie Deng, Jian Guo, Wei Liu*

School of Energy and Power Engineering, Huazhong University of Science and Technology, Wuhan 430074, China

ARTICLE INFO

Article history:
Received 27 February 2011
Accepted 5 May 2011
Available online 12 May 2011

Keywords:
Heat transfer enhancement
Flow resistance
Turbulent flow
Conical strip inserts
Thermo-hydraulic performance
Numerical simulation

ABSTRACT

In an attempt to enhance the heat transfer without significant increase of pressure drop, we developed a conical strip turbulator in the present work. Characteristics of heat transfer rate, flow resistance, and overall thermo-hydraulic performance of turbulent flow in a circular tube fitted with the conical strip inserts were investigated through numerical simulation. The computation results show that the maximal friction factor of the enhanced tube is increased by ~10 times (f = 0.062–0.36); while the Nusselt number is augmented by ~5 times (Nu = 98.35–400.41) as that of the smooth tube. The value of performance evaluation criterion (PEC) lies in the range of 1.67–2.06, which demonstrates that the conical strip insert has a very good thermo-hydraulic performance. Effects of the geometric parameters of the conical strip were also examined. The numerical results indicate that larger slant angle and small pitch can effectively enhance the heat transfer rate, but also increase the flow resistance. Moreover, it is shown that the Nusselt number and friction factor are more sensitive to the slant angle than the inserts pitch. Comparatively steady thermo-hydraulic performance can be obtained at a moderate slant angle together with a small pitch. In addition to those good performances, the conical strip is also easy to fabricate. Thus, it is a promising tube insert which would be widely used in heat transfer enhancement of turbulent flow.

1. Introduction

Shell-and-tube heat-exchangers are widely applied in numerous industrial fields such as power generation, air-conditioning, petro-chemical industry, etc. In those devices, heat is transferred from the warm fluid to the cold fluid via the solid walls. If the heat transfer rate is not so high, some approach is usually needed to enhance the heat transfer process. Researchers throughout the world have made great efforts to the development of heat transfer augmentation techniques [1], which are classified either as passive or active. For the passive techniques, direct application of external power is not needed. Therefore, they are more frequently applied in practical situations. Various kinds of tube inserts, such as the twisted tape, conical ring, porous media inserts, etc., belong to the passive techniques [2]. By using a tube insert, the swirl flow can be intensified and the thickness of the thermal boundary layer can be also reduced. Thus, heat transfer rate can be increased. However, this is realized at the cost of an increase in the flow resistance. In order to comprehensively evaluate the overall thermo-hydrodynamic performance of different enhancement techniques, a variety of performance evaluation criteria (PEC) were proposed. One of the most frequently used is shown below [3]

$$\mathrm{PEC} = \frac{\mathrm{Nu}/\mathrm{Nu}_0}{(f/f_0)^{1/3}} \tag{1}$$

where Nu and Nu_0 are the Nusselt numbers of the enhanced tube and smooth tube, respectively; while f and f_0 are the friction factors of the enhanced tube and smooth tube, respectively. From the above formula one can see that the PEC value of an effective enhancement technique should be at least larger than unity. The larger the PEC value, the better the overall thermo-hydraulic performance is. Meanwhile, Eq. (1) also indicates that a larger heat transfer rate does not mean a better overall performance. Therefore, enough attention should be paid to flow resistance increase when developing a new heat transfer enhancement technique.

Up to now, many kinds of tube inserts have been developed by researchers [4]. For instance, the twisted tape is the most widely used one. This is mainly due to its steady performance. In addition, the twisted tape has a simple configuration and easy to install and disassemble. The main mechanism of heat transfer augmentation by using a twisted tape is that it can generate swirls which enhance

* Corresponding author. Tel.: +86 27 87542618; fax: +86 27 87540724.
E-mail addresses: faw@mail.hust.edu.cn, w_liu@hust.edu.cn (W. Liu).

1359-4311/$ – see front matter © 2011 Elsevier Ltd. All rights reserved.
doi:10.1016/j.applthermaleng.2011.05.007

fluid mixing of the near-wall and central regions [5–8]. As mentioned above, the thermal improvements are always accompanied by increased pressure drop. To optimize the overall thermo-hydraulic performance of tubes fitted with twisted tapes, a great many researchers have made improvements or modifications on the conventional twisted tape. To name a few, segmented twisted tapes [9,10], broken twisted tapes [11], serrated twisted tape [12], and helical screw-tape [13–15], etc. were designed and investigated in the past decade.

In addition to the twisted tape and its modifications, many other types of tube inserts were developed and studied, such as coiled wire turbulators [16–18], circular cross sectional rings [19], porous medium inserts [20,21], conical-ring turbulators [22–24], etc. Another direction of study is the combination of two enhancement techniques. For example, Promvonge investigated the thermal augmentation in circular tube with twisted tape and wire coil turbulators [25]. Also, Promvonge and Eiamsa-ard studied the heat transfer enhancement in a tube with combined conical-nozzle inserts and swirl generator [26], and combined conical-ring and twisted-tape insert [27]. Those works showed that heat transfer can be enhanced to some extent by the combined methods, but the flow resistance was also increased.

Although tremendous efforts have been made to enhance the convective heat transfer in tubes and ducts, techniques which can obtain a good heat transfer performance together with a relatively low flow resistance are still admirable. To achieve these aims, we develop a conical strip insert in the present work. The geometry of this enhancement element is depicted in Fig. 1(a). For this technique, the blocking area is small in the core flow region where the fluid velocity is relatively high; while in the vicinity of the boundary layers, the blocking area is relatively large. Thus, this method can have a good enhancement effect with a relatively low flow resistance. In other words, it is expected to be capable of achieving a high PEC value. In the present paper, we investigate the heat transfer and flow resistance characteristics of turbulent flow in a circular tube fitted with the conical strip inserts through numerical simulation. Our main attention will be paid to the effects of two parameters, i.e., the slant angle and pitch of the conical strip.

2. Numerical modeling

2.1. Physics model

A schematic of the physical model is shown in Fig. 1. The conical strip is a quarter of the surface of a cone. It connects with a central rod of 1 mm diameter. The length and thickness of the conical strip are 16 mm and 1 mm, respectively. The effect of different combinations of the slant angle ($\alpha = 10$, 20 and 30°) and pitch ($S = 30$, 45 and 60 mm) will be investigated in the present work. The length and inner diameter of the tube are $L = 500$ mm and $D = 19.6$ mm, respectively. The length of the investigated region is $L_0 = 300$ mm, with an upstream section of $L_1 = 100$ mm and a downstream section of $L_2 = 100$ mm. Air is selected as the working fluid. Heat conduction in the conical strips and central rod is neglected. The thickness of solid wall is also not considered.

2.2. Governing equations

In the present work, we are to investigate the turbulent heat transfer in the circular tube, with a range of the Reynolds number of 12,000–42,000. The corresponding inlet velocity is 8.9–31.3 m/s. Usually, when the working fluid is air, the suggested flow velocity range is around 8.0–30.0 m/s in the tube side of a real heat exchanger. Thus, the selection of the Reynolds number in this paper is reasonable.

The problem under consideration is assumed to be three-dimensional, turbulent and steady. The following assumptions are made for the derivation of governing equations: 1) the physical properties of fluid are constant; 2) fluid is incompressible, isotropic and continuous; 3) fluid is Newtonian fluid; 4) the effect of gravity is negligible. Equations of continuity, momentum and energy for the fluid flow are given below in a tensor form,

Continuity equation:

$$\frac{\partial(\rho u_i)}{\partial x_i} = 0 \tag{2}$$

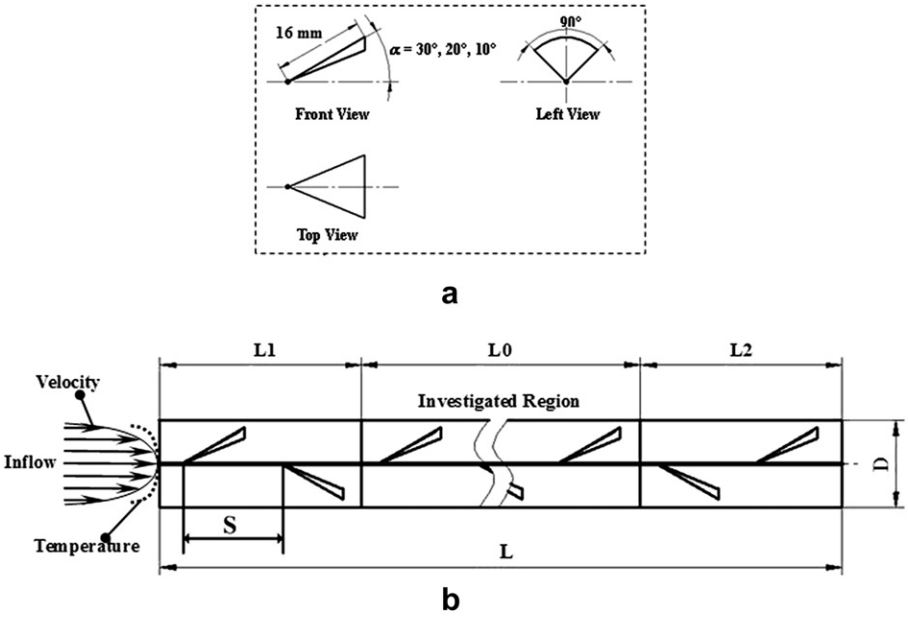

Fig. 1. (a) Geometry of the conical strip insert, and (b) schematic of a circular tube fitted with conical strip inserts.

Momentum equation:

$$\frac{\partial}{\partial x_j}(\rho u_i u_j) = -\frac{\partial p}{\partial x_i} + \frac{\partial}{\partial x_j}\left[\mu\left(\frac{\partial u_i}{\partial x_j} + \frac{\partial u_j}{\partial x_i}\right) - \frac{2}{3}\mu\frac{\partial u_k}{\partial x_k}\delta_{ij}\right] \quad (3)$$

Energy equation:

$$\frac{\partial}{\partial x_j}\left(\rho u_j C_P T - k\frac{\partial T}{\partial x_j}\right) = u_j\frac{\partial p}{\partial x_j} + \left[\mu\left(\frac{\partial u_i}{\partial x_j} + \frac{\partial u_j}{\partial x_i}\right) - \frac{2}{3}\mu\frac{\partial u_k}{\partial x_k}\delta_{ij}\right] \quad (4)$$

In the present study, k-ε RNG turbulence model is used as follows:

$$\frac{\partial(\rho k)}{\partial t} + \frac{\partial(\rho k u_i)}{\partial x_i} = \frac{\partial}{\partial x_j}\left[\alpha_k \mu_{\text{eff}}\frac{\partial k}{\partial x_j}\right] + G_k - \rho\varepsilon \quad (5)$$

$$\frac{\partial(\rho\varepsilon)}{\partial t} + \frac{\partial(\rho\varepsilon u_i)}{\partial x_i} = \frac{\partial}{\partial x_j}\left[\alpha_k \mu_{\text{eff}}\frac{\partial \varepsilon}{\partial x_j}\right] + \frac{C_{1\varepsilon}^{*}\varepsilon}{k}G_k - C_{2\varepsilon}\rho\frac{\varepsilon^2}{k} \quad (6)$$

where ρ is the density of air; u, v, w refer to the flow velocities in x, y, z directions, respectively; c_p is the specific heat at constant pressure; λ is thermal conductivity; μ is dynamic viscosity; k is turbulent kinetic energy; ε is dissipation rate; In Eqs. (5) and (6), $\mu_{\text{eff}} = \mu + \mu_t$, $\mu_t = \rho C_\mu \frac{k^2}{\varepsilon}$, $C_\mu = 0.0845$, $\alpha_k = \alpha_\varepsilon = 1.39$, $C_{1\varepsilon}^{*} = C_{1\varepsilon} - \eta\left(1 - \frac{\eta}{\eta_0}\right)/(1 + \beta\eta^3)$, $C_{1\varepsilon} = 1.42$, $C_{2\varepsilon} = 1.68$, $\eta_0 = 4.377$, $\eta = (2E_{ij}\cdot E_{ij})^{1/2}\frac{k}{\varepsilon}$, $E_{ij} = \frac{1}{2}\left(\frac{\partial u_i}{\partial x_j} + \frac{\partial u_j}{\partial x_i}\right)$, $\beta = 0.012$.

2.3. Boundary conditions

The constant heat flux condition is specified on the tube wall and the value of heat flux depends on the Reynolds number. By this way we can control the temperature increases of the fluid to be approximately the same. At the tube inlet, fully developed flow and temperature boundary conditions are applied. The inlet velocity and temperature profiles were obtained via the following scheme. First, we used uniform inlet velocity and temperature profiles for the smooth tube and conducted one computation. Then, re-computation was performed using the outlet velocity and temperature profiles of the first time. After several times of computation applying this approach, fully developed flow and temperature profiles can be obtained. An example of Re = 24,000 is given in Fig. 2. From Fig. 2(a) it is clearly seen that the superposition of velocity profiles at the inlet and outlet of the tube is quite well. Meanwhile, after subtracting a constant (25.922 K), the temperature profile at the outlet matches very well with that at the inlet, as shown in Fig. 2(b).

At the outlet, a pressure-outlet condition is used. On the tube walls, and the surfaces of the conical strips and central rod, no slip conditions are imposed.

2.4. Computation scheme and validation

Fig. 3 schematically shows the meshes generation of the computation domain. Rectangular and triangular cells were used to mesh the surfaces of tube wall and inserts, respectively; while for the internal space of the circular tube, tetrahedral meshes were adopted. Local grid refinement was applied in the boundary layers. Adaptive grid refinement was also performed in the preliminary computations. The grid independence has been checked by using different grid systems and around 2,000,000 grids are employed to conduct the following computations.

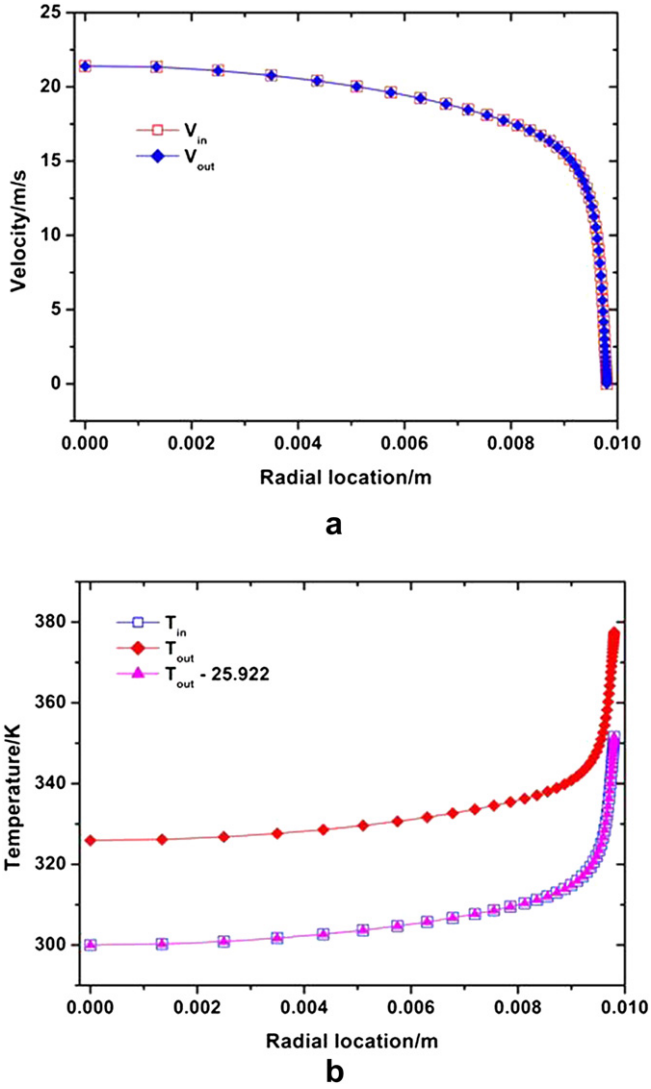

Fig. 2. Fully developed flow and temperature boundary conditions applied at the tube inlet: (a) velocity, and (b) temperature.

All the above-mentioned equations accompanied by boundary conditions are discretized using finite volume formulation. In the equations, the momentum, turbulent kinetic energy, turbulent dissipation rate and temperature terms are modeled by the second-order upwind scheme. The numerical solution procedure adopts the 'SIMPLE' algorithm. The convergent criterion is set as the relative residual of all variables to be less than 10^{-6}. The commercial CFD software package, Fluent 6.3, is used for the numerical simulation.

To verify the numerical method described above, we compared the computational results with the well known empirical formulas for fully developed turbulent flows. From the comparison presented in Fig. 4, it is seen that the agreement between the CFD results and empirical correlations is quite well. Therefore, the present numerical predictions have reasonable accuracy.

3. Results and discussions

3.1. Calculations of the Nusselt number, friction factor and PEC

After computing velocity and temperature fields, heat transfer coefficient between the fluid and wall can be calculated as

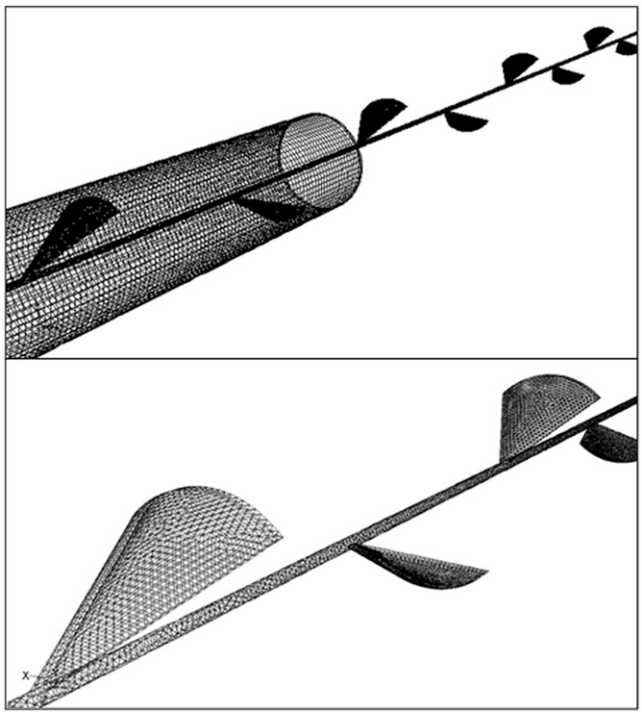

Fig. 3. Meshes generation of the computation domain.

$$h = \frac{q}{T_w - T_m} \tag{7}$$

where T_m is bulk temperature of the fluid:

$$T_m = \frac{\int_0^R uTrdr}{\int_0^R urdr} \tag{8}$$

The Nusselt number and friction factor can be calculated as

$$\mathrm{Nu} = \frac{hD}{\lambda} \tag{9}$$

$$f = \frac{2\Delta \mathrm{PD}}{L\rho u_m^2} \tag{10}$$

where u_m is the mean velocity of the transverse plane in the tube.

To evaluate the effect of heat transfer enhancement under given pumping power, the performance evaluation criterion (PEC) is employed, as shown in Eq. (1).

3.2. Variation of the Nusselt number

The variations of the Nusselt number versus the Reynolds number are shown in Figs. 5–7 for conical strip inserts of different pitches. It is noted that the Nusselt number is augmented by around 5 times as that of the smooth tube. This verifies that the conical strip has a good effect of heat transfer enhancement. Moreover, some general tendencies can be drawn from Figs. 5–7. First, the Nusselt number increases with the increase of the Reynolds number. Second, the Nusselt number increases with the increase of the slant angle of conical strip when the Reynolds number and the

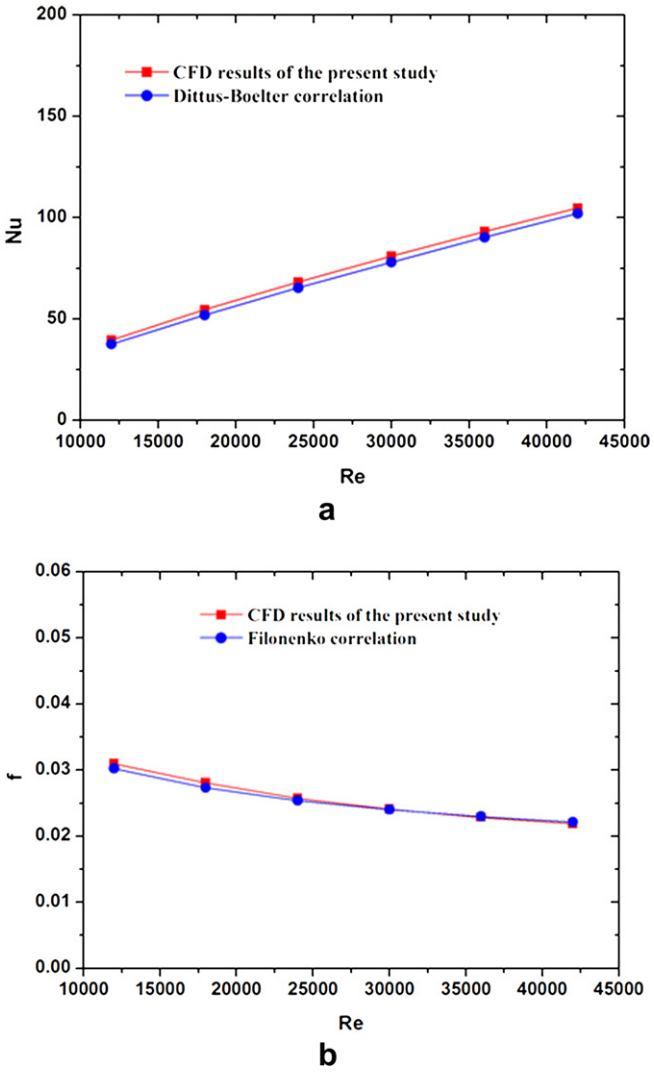

Fig. 4. Data verification of the Nusselt number Nu and friction factor *f* for smooth tube: (a) Nu, and (b) *f*.

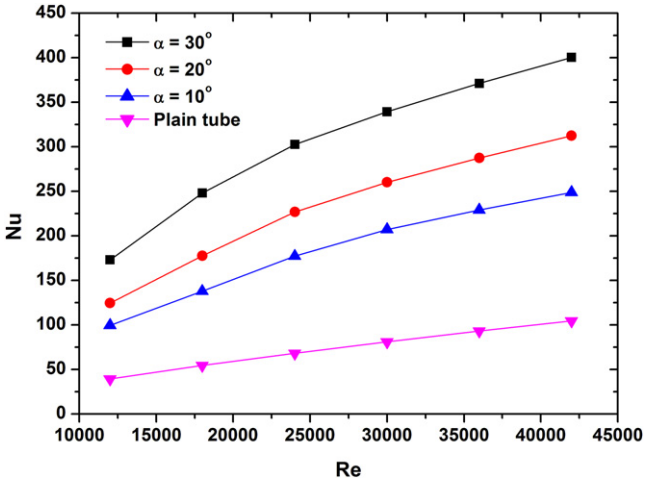

Fig. 5. Variation of the Nusselt number with Reynolds number for different slant angles. The pitch of the inserts is 30 mm in this case.

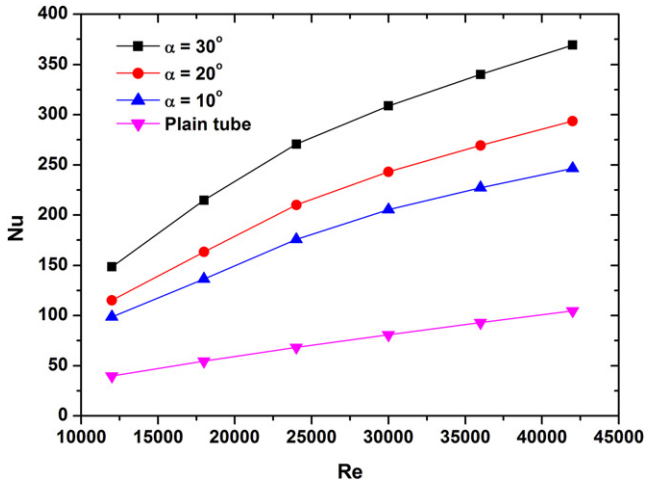

Fig. 6. Variation of the Nusselt number with Reynolds number for different slant angles. The pitch of the inserts is 45 mm in this case.

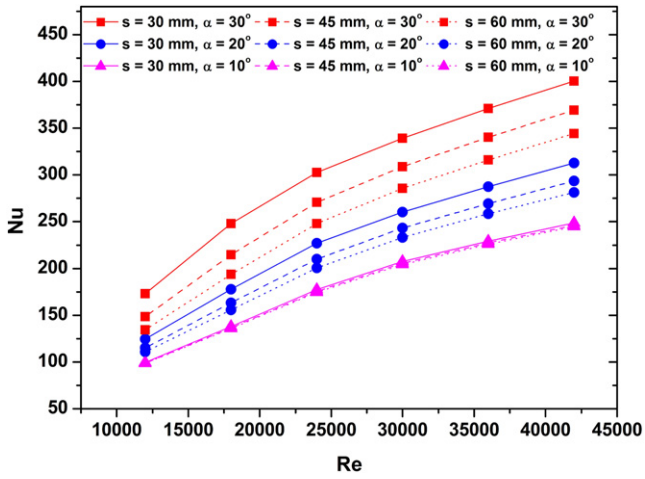

Fig. 8. Variation of the Nusselt number with Reynolds number for different slant angles and pitches.

inserts pitch are the same. In other words, the larger the slant angle, the better the convective heat transfer is.

To facilitate examining the effect of inserts pitch on the heat transfer enhancement, we plot all those data in Fig. 8. From this figure, one can see that when the slant angle is 30°, a relatively small pitch has a much better effect on heat transfer enhancement, which is clearly illustrated by the three red lines in Fig. 8. However, with the decrease of the slant angle ($\alpha = 20°$), the impact of inserts pitch grows not so significant. When $\alpha = 10°$, the influence of inserts pitch becomes very limited, as shown in Fig. 8. (For interpretation of the references to colour in this figure legend, the reader is referred to the web version of this article.)

3.3. Variation of the friction factor

Figs. 9–11 depict the variations of the friction factor versus the Reynolds number for conical strip inserts of different pitches. It is noted that the maximal friction factor of the enhanced tube is about 10 times that of the smooth tube. Contrast with the Nusselt number, the friction factor decreases with the increase of the Reynolds number. Moreover, the friction factor increases with the increase of the slant angle of conical strip when the Reynolds

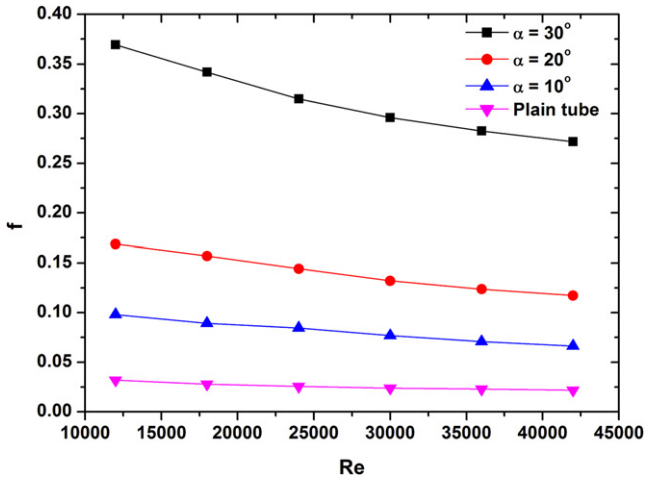

Fig. 9. Variation of the friction factor with Reynolds number for different slant angles. The pitch of the inserts is 30 mm in this case.

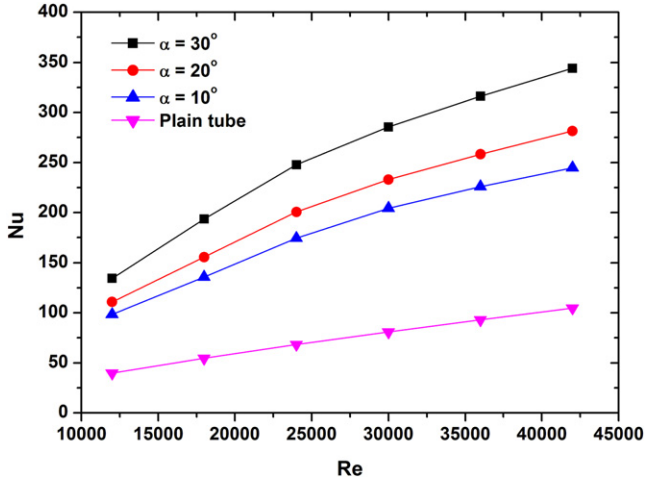

Fig. 7. Variation of the Nusselt number with Reynolds number for different slant angles. The pitch of the inserts is 60 mm in this case.

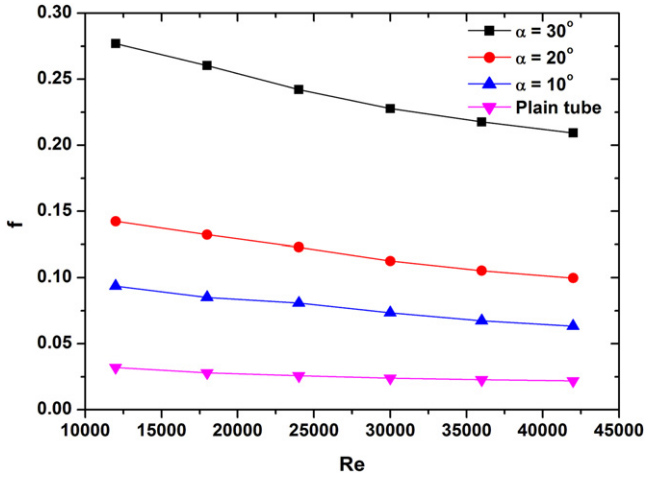

Fig. 10. Variation of the friction factor with Reynolds number for different slant angles. The pitch of the inserts is 45 mm in this case.

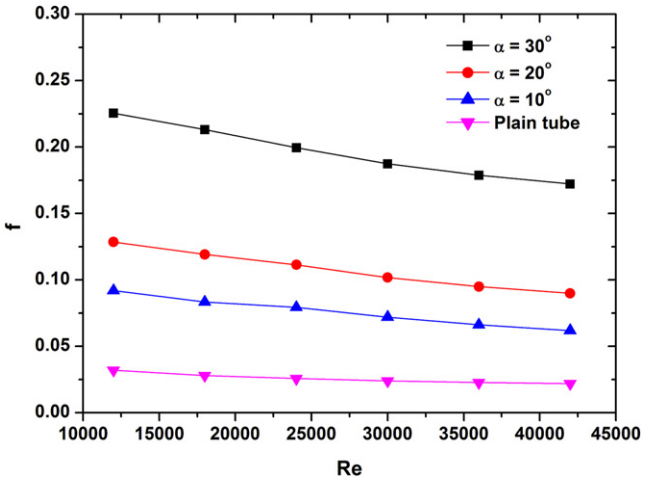

Fig. 11. Variation of the friction factor with Reynolds number for different slant angles. The pitch of the inserts is 60 mm in this case.

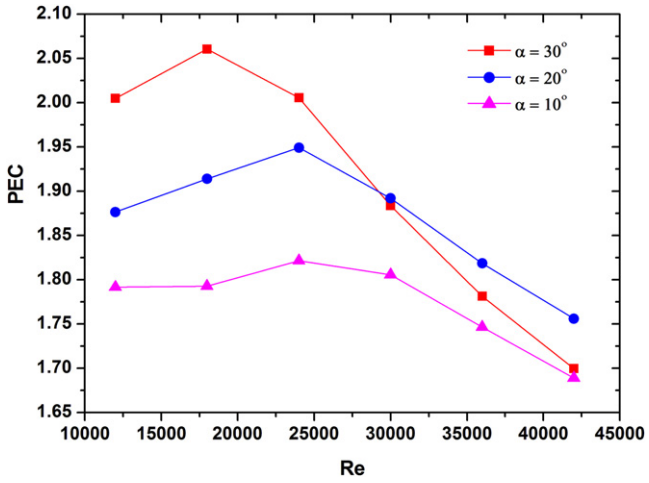

Fig. 13. Variation of the PEC value with Reynolds number for different slant angles. The pitch of the inserts is 30 mm in this case.

number and inserts pitch are the same. In other words, the larger the slant angle, the larger the flow resistance is. This variation tendency is the same as that of the Nusselt number.

Similarly, for a convenience of examining the effect of inserts pitch on the friction factor, we put all the data of Figs. 9–11 in Fig. 12. From this figure, one can see that when the slant angle is 30°, a relatively small pitch results in a much larger friction factor, which is clearly illustrated by the three red lines in Fig. 12. However, with the decrease of the slant angle ($\alpha = 20°$), the impact of inserts pitch is also reduced. When $\alpha = 10°$, the influence of inserts pitch is very weak, as shown in Fig. 12. (For interpretation of the references to colour in this figure legend, the reader is referred to the web version of this article.)

3.4. Variation of the performance evaluation criteria (PEC)

The variation tendency of performance evaluation criteria (PEC) versus the Reynolds number is shown in Figs. 13–15 for conical trip inserts of different pitches. From these figures it is seen that the PEC value lies in the range of 1.67–2.06, which demonstrates that the conical strip insert has a very good thermo-hydraulic performance. Different from the Nusselt number and friction factor, the variation

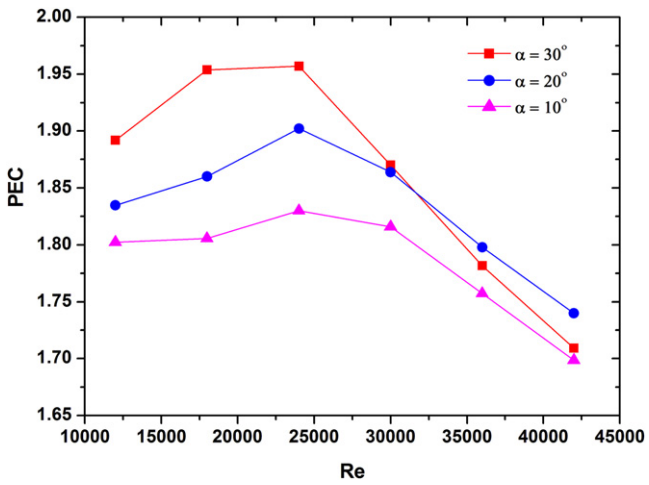

Fig. 14. Variation of the PEC value with Reynolds number for different slant angles. The pitch of the inserts is 45 mm in this case.

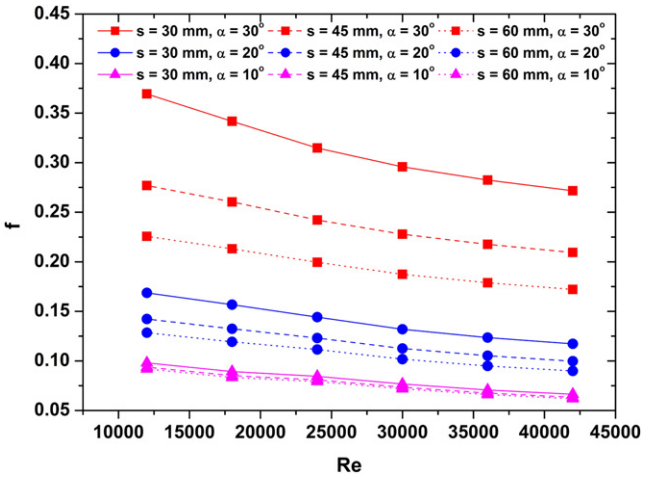

Fig. 12. Variation of the friction factor with Reynolds number for different slant angles and pitches.

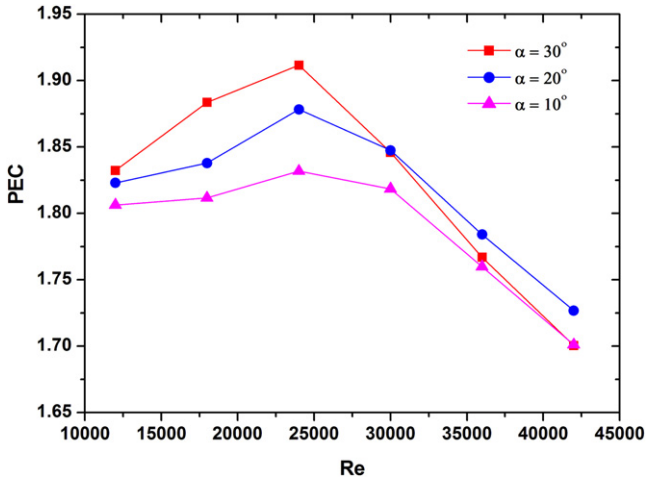

Fig. 15. Variation of the PEC value with Reynolds number for different slant angles. The pitch of the inserts is 60 mm in this case.

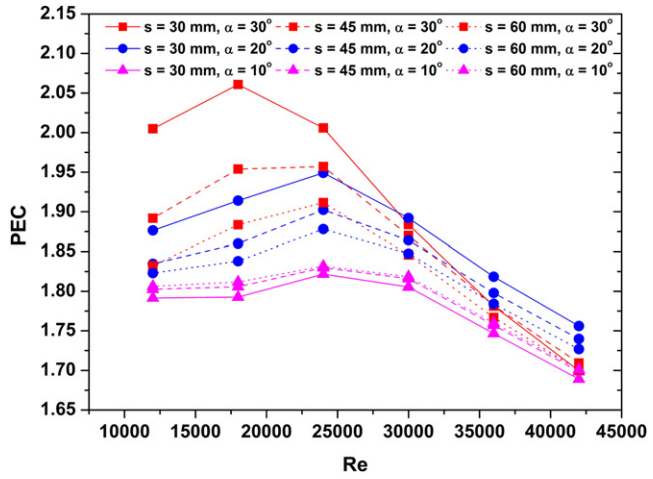

Fig. 16. Variation of the PEC value with Reynolds number for conical strip inserts of different slant angles and pitches.

of PEC is not monotonically. In other words, it first increases with the increase of the Reynolds number, and then decreases with the further increase of the Reynolds number. At a moderate Re, the PEC reaches its peak value. Furthermore, the PEC of a relatively small pitch decreases more quickly when the Reynolds number is larger than its critical value. Thus, under large Re conditions, the PEC of the case with a small pitch can drop to a value less than that of a large pitch, as shown in Figs. 13–15.

Fig. 16 depicts all the data in Figs. 13–15. From this figure it is clearly seen that when the Reynolds number is small, a better thermo-hydraulic performance can be achieved by using a larger slant angle ($\alpha = 30^\circ$) together with a relatively small pitch ($S = 30$ and 45 mm). However, when the Reynolds number is large, a moderate slant angle ($\alpha = 20^\circ$) together with a short pitch ($S = 30$ mm) should be selected to obtain a largest PEC value. Meanwhile, the PEC values of this combination ($\alpha = 20^\circ$ and $S = 30$ mm) are also relatively high at low Re. Thus, to achieve a relatively good thermo-hydraulic performance over the whole Re range, the best parameter combination should be $\alpha = 20^\circ$ and $S = 30$ mm.

3.5. Discussions

The numerical results demonstrated that the heat transfer rate and flow resistance depend on the parameters combination of the conical strip. This is because the fluid mixing, boundary layer disturbing, and convective heat transfer have close relation to those geometric parameters. Thus, we present the flow and temperature fields of the case at Re = 24,000 as example to analyze the effect of the geometric parameters, as shown in Figs. 17 and 18, respectively. From Fig. 17(a)–(c), it is clearly seen that the fluid mixing and boundary disturbing are greatly intensified when the slant angle of the conical strip is increased from 10° to 30°. Thus, the flow boundary layer becomes thinner at larger slant angles. This will result in a significant increase in the friction factor, as have been shown in Figs. 9–12. Similarly, due to the good effect of fluid mixing and boundary disturbing at large slant angle, the temperature field

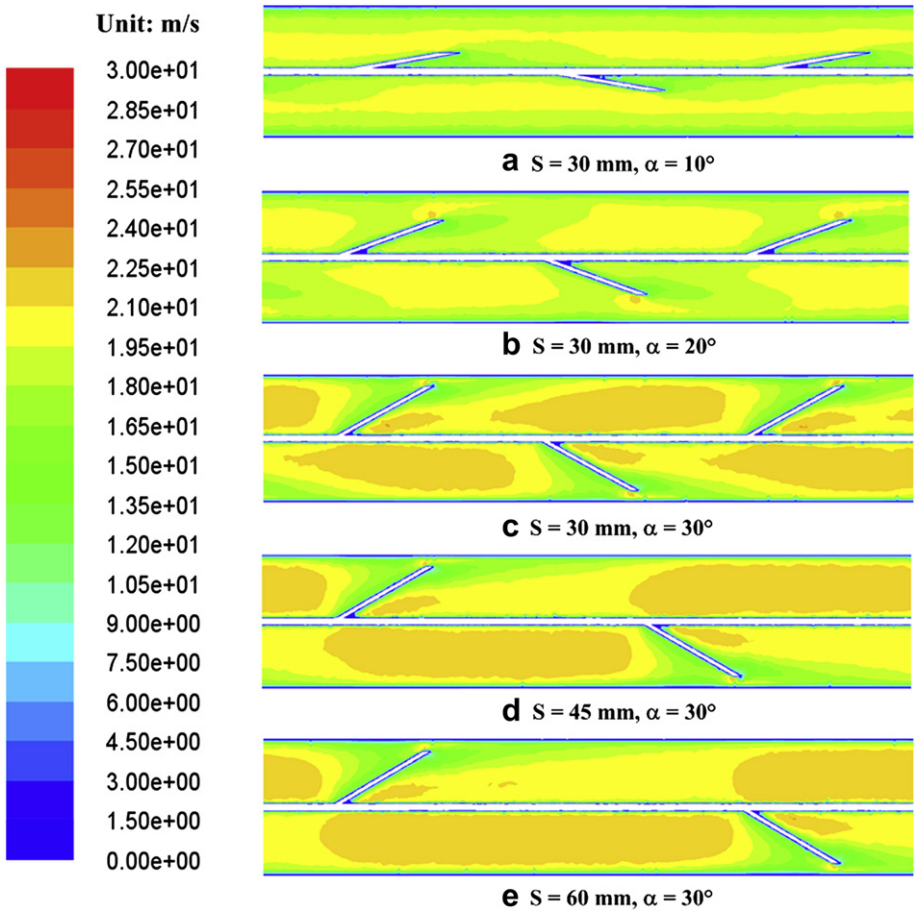

Fig. 17. Velocity contours at Re = 24,000: (a) $S = 30$ mm, $\alpha = 10^\circ$, (b) $S = 30$ mm, $\alpha = 20^\circ$, (c) $S = 30$ mm, $\alpha = 30^\circ$, (d) $S = 45$ mm, $\alpha = 30^\circ$, and (e) $S = 60$ mm, $\alpha = 30^\circ$.

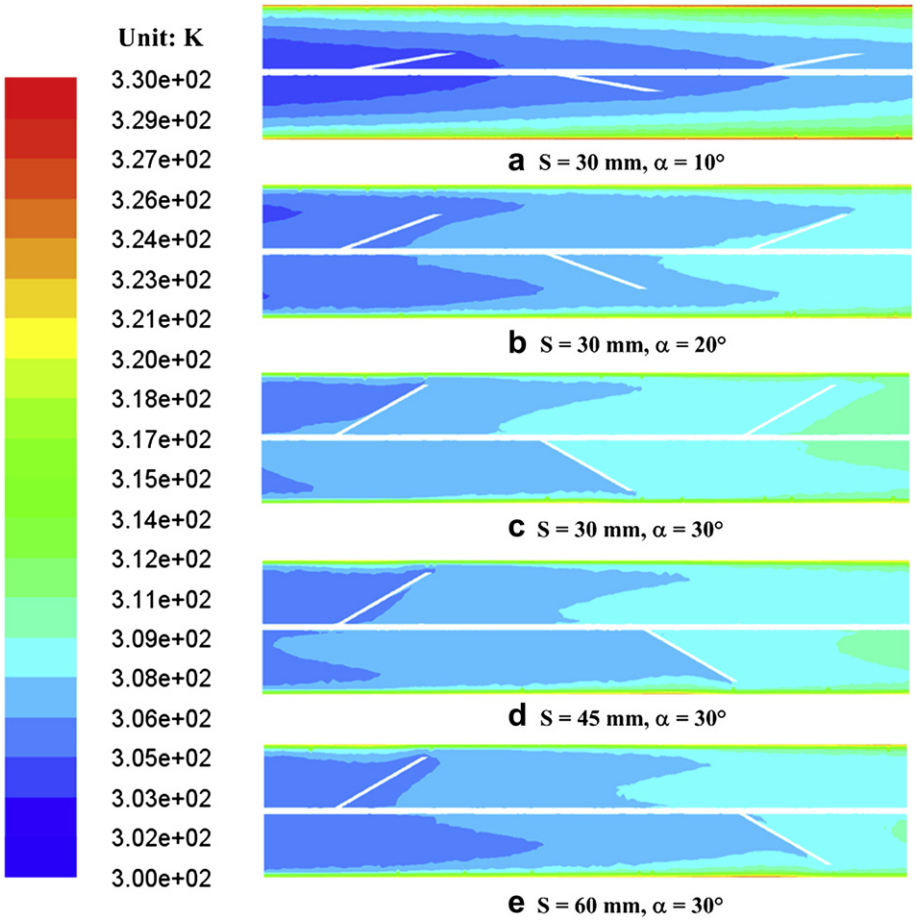

Fig. 18. Temperature contours at Re = 24,000: (a) $S = 30$ mm, $\alpha = 10°$, (b) $S = 30$ mm, $\alpha = 20°$, (c) $S = 30$ mm, $\alpha = 30°$, (d) $S = 45$ mm, $\alpha = 30°$, and (e) $S = 60$ mm, $\alpha = 30°$.

grows more uniform in the core flow region, and the temperature gradient becomes larger in the boundary layer simultaneously. Therefore, heat transfer will be substantially enhanced and the outlet temperature will be higher at large slant angles of the conical strip.

Effects of the slant angle on the Nusselt number and friction factor can also be explained by the field synergy theory which was first proposed by Guo [28–30], further developed by Tao et al. [31,32] and Liu et al. [33,34], and applied by other researchers for heat exchanger optimization design [35]. This principle indicates that the heat transfer rate depends not only on the magnitudes of the flow velocity and temperature gradient but also on their synergy [28–30]. According to the field synergy principle, the better the coordination of velocity and heat flow (temperature gradient) fields, the higher the convective heat transfer rate is. For the present study, when the slant angle of the conical strip is larger, the coordination of velocity and heat flow fields is better. Thus, heat transfer enhancement is more significant. However, according to the developed field synergy theory by Liu et al. [33,34], when the slant angle of the conical strip is larger, the field synergy angle between the velocity vector and pressure gradient becomes larger, which leads to an increment in the flow resistance. This implies that the coordination of velocity and driving force (pressure gradient) fields becomes worse. Therefore, the friction factor increases more significant as compared with that of small slant angle. The overall thermo-hydraulic performance depends on a compromise between those two sides. As has been shown in Fig. 16, a moderate slant angle is beneficial for obtaining a relatively high PEC value over the whole Re range under investigation.

Explanation of the effect of inserts pitch is relatively simple. When the inserts pitch is small, more insert elements could be added into the investigated region. Thus, the flow resistance will be increased but heat transfer will also be enhanced, as shown in Fig. 17(c)–(e) and Fig. 18(c)–(e).

As for the PEC value, its variation tendency is more complex. This is because it depends on the Nusselt number and friction factor of the enhanced tube and smooth tube simultaneously. In more details, the PEC value is proportional to the ratio, Nu/Nu_0, and inversely proportional to the ratio $(f/f_0)^{1/3}$. From Figs. 8 and 12, we know that the Nusselt number and friction factor are more sensitive to the slant angle than the inserts pitch. The physical mechanism is that, the slant angle can change the flow direction of the fluid, which disturbs the flow and thermal boundaries. When the slant angle is larger, the disturbances of the boundaries are more intensive. Thus, the Nusselt number and friction factor will change substantially. As for the effect of the inserts pitch, since it almost does not change the flow direction, and only differs in the number of turbulators, the Nusselt number and friction factor are not so sensitive to the inserts pitch as the slant angle. Therefore, comparatively steady performance is obtained at a moderate slant angle ($\alpha = 20°$) together with a small pitch ($S = 30$ mm).

4. Conclusions

A conical strip insert was developed to enhance convective heat transfer of turbulent flow in a circular tube. Characteristics of the Nusselt number, friction factor, and performance evaluation criterion were investigated through numerical simulation. The

computation results show that the Nusselt number is augmented by around 5 times that of the smooth tube, which confirms that the conical strip has a good effect of heat transfer enhancement. The maximal friction factor of the enhanced tube is around 10 times that of the smooth tube. The PEC value lies in the range of 1.67–2.06, which demonstrates that the conical strip insert has a very good thermo-hydraulic performance. The peak value of PEC appears at a moderate Reynolds number.

Effects of the geometric parameters of the conical strip were also examined. The numerical results indicate that larger slant angle and small pitch can effectively enhance the heat transfer rate, but also increase the flow resistance. Moreover, it is shown that the Nusselt number and friction factor are more sensitive to the slant angle than the inserts pitch. Comparatively steady thermo-hydraulic performance is obtained at a moderate slant angle ($\alpha = 20^\circ$) together with a small pitch ($S = 30$ mm).

In addition to those good performances, the conical strip is also easy to fabricate. Thus, it is a promising tube insert which can be widely used in heat transfer enhancement of turbulent flow. Experimental investigation will be carried out in our group, which will be reported in our future paper.

Acknowledgments

This work was supported by the Natural Science Foundation of China (No.51036003, No.51076054) and the National Key Basic Research Development Program of China (No.2007CB206903).

Nomenclature

c_p	the specific heat at constant pressure, kJ/kg·K
D	the tube diameter, m
f	friction factor
h	the average heat transfer coefficient in the tube, W/m^2·K
k	turbulent kinetic energy, m^2/s^2
L	the full length of tube, m
L_0	the length of investigated region, m
L_1	the length before investigated region, m
L_2	the length after investigated region, m
Nu	average Nusselt number
p	pressure, N/m^2
q	heat transfer rate per unit tape length, W/m
Re	the Reynolds number
S	pitch of conical strip, m
T	temperature, K
u	flow velocity in x direction, m/s
v	flow velocity in y direction, m/s
w	flow velocity in z direction, m/s

Greek symbols

α	slant angle ($^\circ$)
ρ	density of air, kg/m^3
λ	thermal conductivity, W/m·K
ε	turbulent dissipation rate, m^2/s^3

Subscripts

0	plain tube
m	mean
w	wall

References

[1] A.E. Bergles, ExHFT for fourth generation heat transfer technology, Experimental Thermal and Fluid Science 26 (2002) 335–344.
[2] V. Zimparov, Energy conservation through heat transfer enhancement techniques, International Journal of Energy Research 26 (2002) 675–696.
[3] R.L. Webb, Performance evaluation criteria for use of enhanced heat transfer surfaces in heat exchanger design, International Journal of Heat and Mass Transfer 24 (1981) 715–726.
[4] L. Wang, B. Sunden, Performance comparison of some tube inserts, International Communications in Heat and Mass Transfer 29 (2002) 45–56.
[5] P. Naphon, Heat transfer and pressure drop in the horizontal double pipes with and without twisted tape insert, International Communications in Heat and Mass Transfer 33 (2006) 166–175.
[6] R.M. Manglik, A.E. Bergles, Heat transfer and pressure drop correlations for twisted tape inserts in isothermal tubes: Part I–laminar flows, Journal of Heat Transfer 115 (1993) 881–889.
[7] R.M. Manglik, A.E. Bergles, Heat transfer and pressure drop correlations for twisted tape inserts in isothermal tubes: part II–transition and turbulent flows, Journal of Heat Transfer 115 (1993) 890–896.
[8] A. Kumar, B.N. Prasad, Investigation of twisted tape inserted solar water heaters–heat transfer, friction factor and thermal performance results, Renewable Energy 19 (2000) 379–398.
[9] S.K. Saha, A. Dutta, S.K. Dhal, Friction and heat transfer characteristics of laminar swirl flow through a circular tube fitted with regularly spaced twisted-tape elements, International Journal of Heat and Mass Transfer 44 (2001) 4211–4223.
[10] S. Eiamsa-ard, C. Thianpong, P. Promvonge, Experimental investigation of heat transfer and flow friction in a circular tube fitted with regularly spaced twisted tape elements, International Communications in Heat and Mass Transfer 33 (2006) 1225–1233.
[11] S.W. Chang, T.L. Yang, J.S. Liou, Heat transfer and pressure drop in tube with broken twisted tape insert, Experimental Thermal and Fluid Science 32 (2007) 489–501.
[12] S.W. Chang, Y.J. Jan, J.S. Liou, Turbulent heat transfer and pressure drop in tube fitted with serrated twisted tape, International Journal of Thermal Science 46 (2007) 506–518.
[13] P. Sivashanmugam, S. Suresh, Experimental studies on heat transfer and friction factor characteristics of laminar flow through a circular tube fitted with helical screw-tape inserts, Applied Thermal Engineering 26 (2006) 1990–1997.
[14] P. Sivashanmugam, S. Suresh, Experimental studies on heat transfer and friction factor characteristics of turbulent flow through a circular tube fitted with regularly spaced helical screw-tape inserts, Applied Thermal Engineering 27 (2007) 1311–1319.
[15] S. Eiamsa-ard, P. Promvonge, Enhancement of heat transfer in a tube with regularly-spaced helical tape swirl generators, Solar Energy 78 (2005) 483–494.
[16] P. Promvonge, Thermal performance in circular tube fitted with coiled square wires, Energy Conversion and Management 49 (2008) 980–987.
[17] A. Carcia, J.P. Solano, P.G. Vicente, A. Viedma, Enhancement of laminar and transitional flow in tubes by means of wire coil inserts, International Journal of Heat and Mass Transfer 50 (2007) 3176–3189.
[18] K. Yakut, B. Sahin, The effects of vortex characteristics on performance of coiled wire turbulators used for heat transfer augmentation, Applied Thermal Engineering 24 (2004) 2427–2438.
[19] V. Ozceyhan, S. Gunes, O. Buyukalaca, N. Altuntop, Heat transfer enhancement in a tube using circular cross sectional rings separated from wall, Applied Energy 85 (2008) 988–1001.
[20] S.O. Akansu, Heat transfers and pressure drops for porous-ring turbulators in a circular pipe, Applied Energy 83 (2006) 280–298.
[21] Z.F. Huang, A. Nakayama, K. Yang, C. Yang, W. Liu, Enhancing heat transfer in the core flow by using porous medium insert in a tube, International Journal of Heat and Mass Transfer 53 (2010) 1164–1174.
[22] K. Yakut, B. Sahin, Flow-induced vibration analysis of conical rings used for heat transfer enhancement in heat exchangers, Applied Energy 78 (2004) 273–288.
[23] K. Yakut, B. Sahin, C. Celik, S. Canbazoglu, Performance and flow-induced vibration characteristics for conical-ring turbulators, Applied Energy 79 (2004) 65–76.
[24] P. Promvonge, Heat transfer behaviors in round tube with conical ring inserts, Energy Conversion and Management 49 (2008) 8–15.
[25] P. Promvonge, Thermal augmentation in circular tube with twisted tape and wire coil turbulators, Energy Conversion and Management 49 (2008) 2949–2955.
[26] P. Promvonge, S. Eiamsa-ard, Heat transfer enhancement in a tube with combined conical-nozzle inserts and swirl generator, Energy Conversion and Management 47 (2006) 2867–2882.
[27] P. Promvonge, S. Eiamsa-ard, Heat transfer behaviors in a tube with combined conical-ring and twisted-tape insert, International Communications in Heat and Mass Transfer 34 (2007) 849–859.
[28] Z.Y. Guo, D.Y. Li, B.X. Wang, A novel concept for convective heat transfer enhancement, International Journal of Heat and Mass Transfer 41 (1998) 2221–2225.
[29] Z.Y. Guo, Mechanics and control of convective heat transfer-coordination of velocity and heat flow fields, Chinese Science Bulletin 46 (2001) 597–600.
[30] Z.Y. Guo, W.Q. Tao, R.K. Shah, The field synergy principle and its applications in enhancing single phase convective heat transfer, International Journal of Heat and Mass Transfer 48 (2005) 1797–1807.
[31] W.Q. Tao, Z.Y. Guo, B.X. Wang, Field synergy principle for enhancing convective heat transfer-its extension and numerical verification, International Journal of Heat and Mass Transfer 45 (2002) 3849–3856.

[32] W.Q. Tao, Y.L. He, Z.G. Qu, Y.P. Cheng, Application of the field synergy principle in developing new type heat transfer enhanced surfaces, Journal of Enhanced Heat Transfer 11 (2004) 433–449.
[33] W. Liu, Z.C. Liu, Z.Y. Guo, Physical quantity synergy in laminar flow field of convective heat transfer and analysis of heat transfer enhancement, Chinese Science Bulletin 54 (2009) 3579–3586.
[34] W. Liu, Z.C. Liu, S.Y. Huang, Physical quantity synergy in the field of turbulent heat transfer and its analysis for heat transfer enhancement, Chinese Science Bulletin 55 (2010) 2589–2597.
[35] J.F. Guo, M.T. Xu, L. Cheng, The application of field synergy number in shell-and-tube heat exchanger optimization design, Applied Energy 86 (2009) 2079–2087.